The Mine Penetration Sonar System: Design Theory, Design Simulator, Simulations

Reginald D. Hollett

Abstract— **Mine-Penetration Sonar is proposed as a candidate, next-generation minehunter system for enhanced detection and classification of proud and buried seabed mines. The system concept is based on high-resolution target imagery in the low frequency regime (< 30 kHz), by means of backprojection of broadband returns (5-30 kHz), over a broad sector of aspect angles about the target (90-degree sector or more). It is proposed that: 1) in the low frequency regime, the mine casing is readily penetrated, as the thickness is reduced to a fraction of the incident wavelengths; 2) the target scattering is dominated by the coherent field, as the mine is constructed of acoustically-smooth, homogeneous components, both exterior and interior; 3) in the low frequency regime, the coherent field is considerably widened (about the specular), particularly from the interior components, and amenable to broad-sector backprojection. The system design is based on low frequency broadband, broad-sector SAS, capable of high-resolution imagery (typically, 3 cm × 3 cm). The system is envisaged as bi-modal: 1) in its primary mode of operation, the system is run as a strip-map or bottom survey SAS, with initial detection and classification of mine-like objects based on interior imagery; 2) in its secondary mode, the system is run as a spotlight or target-classification SAS on targets of interest, for spectral analysis of response with aspect, template matching, etc. (based on reutilization of the data acquired in primary mode). The system simulations are based on simple modelling of interior components of typical mines and the backprojection of their coherently-scattered returns. The interior components are modelled by means of the boundary element method with the additional simplification of boundary impenetrability (Kirchhoff approx.). It is proposed that the basic acoustic field scattered by the mine interior is sufficiently well represented and that any effects of penetrability are easily evaluated. The simulated target imagery is based on the filtered backprojection algorithm (for echo inversion), and dB levels in the imagery presented as target backscattering strengths, for direct comparison with known bottom backscattering strengths and evaluation of target echo-to-reverberation ratios in the imagery.**

Index Terms— **acoustic imaging, acoustic scattering, acoustic signal processing, synthetic aperture sonar.**

I. Introduction

THE Mine Penetration Sonar (MPS) system is proposed as an enhancement of minehunter system design for detection and classification of seabed influence mines. The MPS system design concept is based on low frequency (LF)[1] high-res. imagery (cm resolution), comparable, in terms of resolution, to high-res. imagery achieved by high frequency (HF)[2] systems [1], [2]. The importance of resolution is evidenced by Fig. 1, in which contemporary LF system performance (9 cm × 9 cm resolution, typically), is compared with MPS system performance (3 cm × 3 cm resolution). The contemporary LF system parameters and MPS system parameters are compared in Table 1.

The MPS system design theory is based on three design principles: 1) imagery by echo inversion; 2) exposure of the target interior by LF penetration of the exterior case; 3) scattering by the LF coherent field from the target interior. In the theory, the target model is based on coherent scattering: the target is fabricated from moulded and machined components, known to be acoustically smooth (physically smooth to the touch); the charge fill is agitated to remove all air inclusions during hardening, consequently, acoustically homogeneous; other components are air filled (arming device, target detection electronics). Incoherent scattering from the target (if any), is neglected.

The MPS system design simulator is based on a simplified target model for coherent scattering; the scattering is modelled by plane-wave reflection and transmission coefficients; the interior components are modelled as acoustically impenetrable. A correction is made for penetrability of the charge fill.

II. The MPS System Design

The MPS system design, basically a synthetic aperture system (SAS) design, is illustrated in Fig. 2. The echoes received along track (pulse compressed), are inverted to a 2-D backscattering function in the slant-range plane, termed the image [3]. The echoes are inverted by means of a backprojector (in the time domain), followed by a filter (in the spatial-frequency domain).

In the imagery, the resolution is defined by

$$\Delta x \Delta y = \frac{\lambda_0}{2\Theta}\frac{c}{2B}, \qquad (1)$$

in which the along-track resolution Δx is expressed in terms of the midband (carrier) wavelength λ_0 and TX/RX sector Θ, and the across-track resolution Δy in terms of the sound speed c and TX/RX bandwidth B [4]. Equation (1) is derived from the equivalent widths of the system impulse response (point-

Manuscript received July 14 2010
R. Hollett is with NURC, Viale S. Bartolomeo, 400, 19126, La Spezia, Italy (e-mail: Hollett@nurc.nato.int).

[1] Below 50 kHz
[2] Above 100 kHz

scatterer response). In (1), the system transfer function is assumed constant over its band-limited support.

The system parameter pair λ_0, B is defined by the target strength (variation with frequency), and penetrability of the exterior case. The parameter Θ is defined by λ_0, B

$$\Theta = \frac{\lambda_0 B}{c}, \qquad (2)$$

by equality of Δx and Δy in (1), for rotational invariance in the imagery.

In the imagery, the target echo-to-reverberation ratio is defined by

$$\mathrm{EL} - \mathrm{RL} = S_\mathrm{T} - S_\mathrm{B}, \qquad (3)$$

in which the ratio is expressed in terms of backscattering strengths, the target backscattering strength S_T and the bottom backscattering strength S_B. In (3), the strength S_T is defined by

$$S_\mathrm{T} = 10\log\left(\left|\frac{\lambda_0}{2\Theta} f_\mathrm{T}\right|^2\right) - 10\log\ \Delta x \Delta y\ , \qquad (4)$$

in which S_T is expressed in terms of the 2-D backscattering function for the target f_T, a function of position x, y. In (4), the function f_T is scaled by the reciprocal of the peak height in the system impulse response, derived for a pulse-compressed, linear frequency-modulated (LFM), TX pulse with parameters λ_0, B.

III. The Simplified Target Penetrability Model

The simplified target penetrability model is illustrated in Fig. 3(a). The penetrability (transmissivity), is modelled by plane-wave transmission coefficients (T), for transmission through a plane layer in water, 1 cm thick.

The T s are illustrated in Fig. 3(b) through (d), for three materials: glass-reinforced plastic (GRP), aluminium, stainless steel. In the LF regime, the limit is reached of magnitude of T equal to 1 and phase 0, termed the acoustic transparency.

IV. The Simplified Target Scattering Model

The simplified target scattering model is illustrated in Fig. 4. The scattering is modelled by plane-wave reflection and transmission coefficients (R, T). The exterior is modelled as acoustically transparent ($R = 0$, $T = 1$). The interior is modelled as an acoustically impenetrable boundary, the main charge as acoustically rigid ($R = 1$, $T = 0$), the safety and arming device (S&AD), the target detection device (TDD), as pressure release ($R = -1$, $T = 0$). The boundary representation is based on a simple boundary element method (BEM).

The target strengths TSs (monostatic), are illustrated in Fig 5 for the Manta mine, and in Fig. 6 for the Murena mine. In the LF regime, the scattering about the specular from the main charge, S&AD, TDD, is broadened out in angle, termed the coherent field.

V. The MPS System Design Simulations

The MPS system design simulations are illustrated in Fig. 1(b) and Fig. 7(a) for the Manta mine, and in Fig. 7(b) for the Murena mine. The system design parameters are tabulated in Table 1. The parameters λ_0, B are defined for frequency coverage from 5 to 30 kHz. At frequencies below 5 kHz, the coherent field from the target interior is diminished; above 30 kHz, the acoustic transparency of the target exterior is diminished. The parameter Θ is defined for quadrant coverage about the target, in excess of (2) by some degrees. The TX pulse type, LFM, is defined for uniform frequency coverage.

The target echo-to-reverberation ratios for interior components are tabulated in Table 2 for the Manta mine, and in Table 3 for the Murena mine. The ratios are defined by the difference in target and bottom backscattering strengths, as in (3). The bottom backscattering strengths are known from experimental measurements reported in the literature on the subject [5].

VI. Summary and Remarks

The MPS system design is based on an LF high-res. imaging based SAS system design. The system design theory is based on fundamental principles: echo inversion, target penetrability, target scattering by the coherent field. The target exterior is penetrated by acoustic transmissions. The target interior is constructed of acoustically smooth, homogeneous parts (for the most part); the scattered field from the target interior is dominated by coherent scattering. In the LF regime, the exterior is rendered acoustically transparent; the coherent field from the interior is broadened out in grazing angle, azimuth, suited to sidescan imagery.

The system design simulator is based on a simplified target model for the coherent field; the scattering is based on plane wave reflection coefficients of ± 1 (Kirchhoff approx.). A correction is made for coefficients of magnitude less than 1. The simulator is utilized as a design tool for investigation of high-res. target imagery, target backscattering strengths, TSs, optimization of parameters.

The LF high-res. target imagery is distinguished by resolution of interior features, the charge fill, arming device, detection device. The delineation of the features is emphasized. The echo-to-reverberation ratios are typified by high values. Improvements in detection, classification (proud and buried targets), automatic target recognition (ATR), reductions in false-alarm rates, are expected.

In terms of imaging performance, the HF regime is less suited to target detection/classification in sidescan imagery. In the HF regime, the coherent scattering from the target is reduced to the specular returns at a few angles (at most); target detection/classification is based on the incoherent field,

weaker than the coherent field and dependent (for the most part), on details in the target construction, amenable to eradication or modification.

In terms of operational effectiveness, imaging based detection/classification is expected to outperform non-imaging based detection/classification [6]. In imaging based detection/classification, operator interaction/interpretation is included. In imaging based detection/classification, the system is operated in two modes: 1) strip-map SAS mode for surveillance, target detection; 2) spotlight SAS mode for classification, in which the data acquired in the strip-map mode are reutilized for application of non-imaging based techniques to detected targets and other objects of interest to the operator.

REFERENCES

[1] A. Bellettini and M. Pinto, "Design and experimental results of a 300-kHz synthetic aperture sonar optimized for shallow-water operations," *IEEE J. Ocean Eng.*, vol. 34, no. 3, pp. 285-293, 2009.

[2] D. Brown, D. Cook, and Jose Fernandez, "Results from a small synthetic aperture sonar," in *Proc. OCEANS*, Boston, MA, 2006, pp. 1-6.

[3] J. A. Fawcett, "Inversion of n-dimensional spherical averages," *SIAM J. Appl. Math.*, vol. 45, no. 2, pp. 336-341, 1985.

[4] L. M. H. Ulander, and H. Hellsten, "A new formula for SAR spatial resolution," *AEU Int. J. Electron. Commun.*, vol. 50, no. 2, pp. 117-121, 1996.

[5] R. J. Urick, *Principles of Underwater Sound*, 3rd ed.. Los Altos, CA: Peninsula Publishing, 1983.

[6] B. H. Houston *et al.*, "Broadband low frequency sonar for non-imaging based identification," in *Proc. OCEANS*, Biloxi, MS, 2002, pp. 383-387.

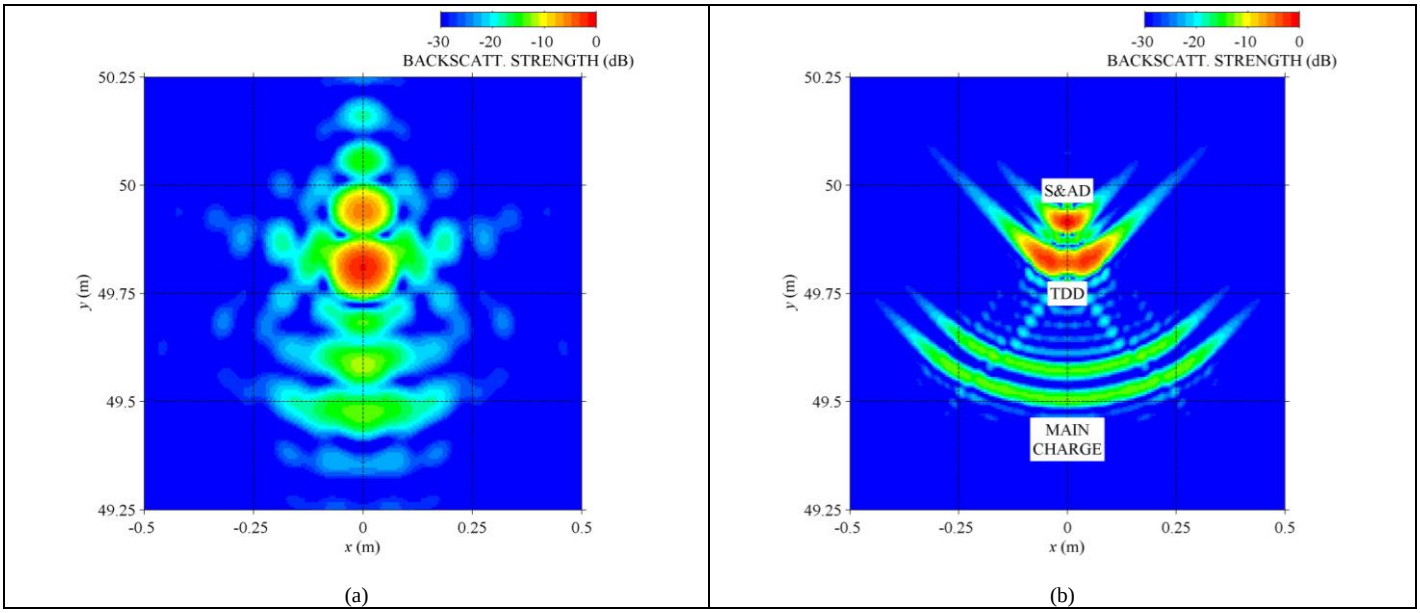

Fig. 1. Comparison of LF system performance, for Manta mine imagery, incident/scattered field at grazing angle of 10 degrees. In (a), contemporary LF system performance; in (b) MPS system.

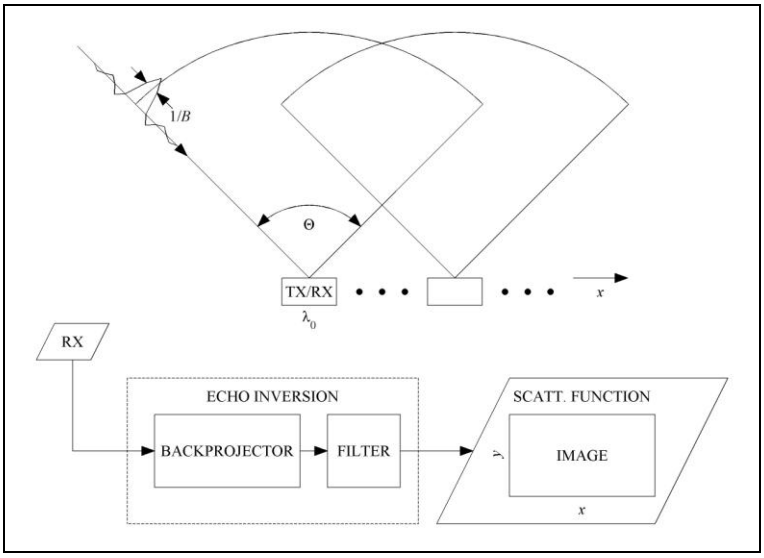

Fig. 2. The MPS system design.

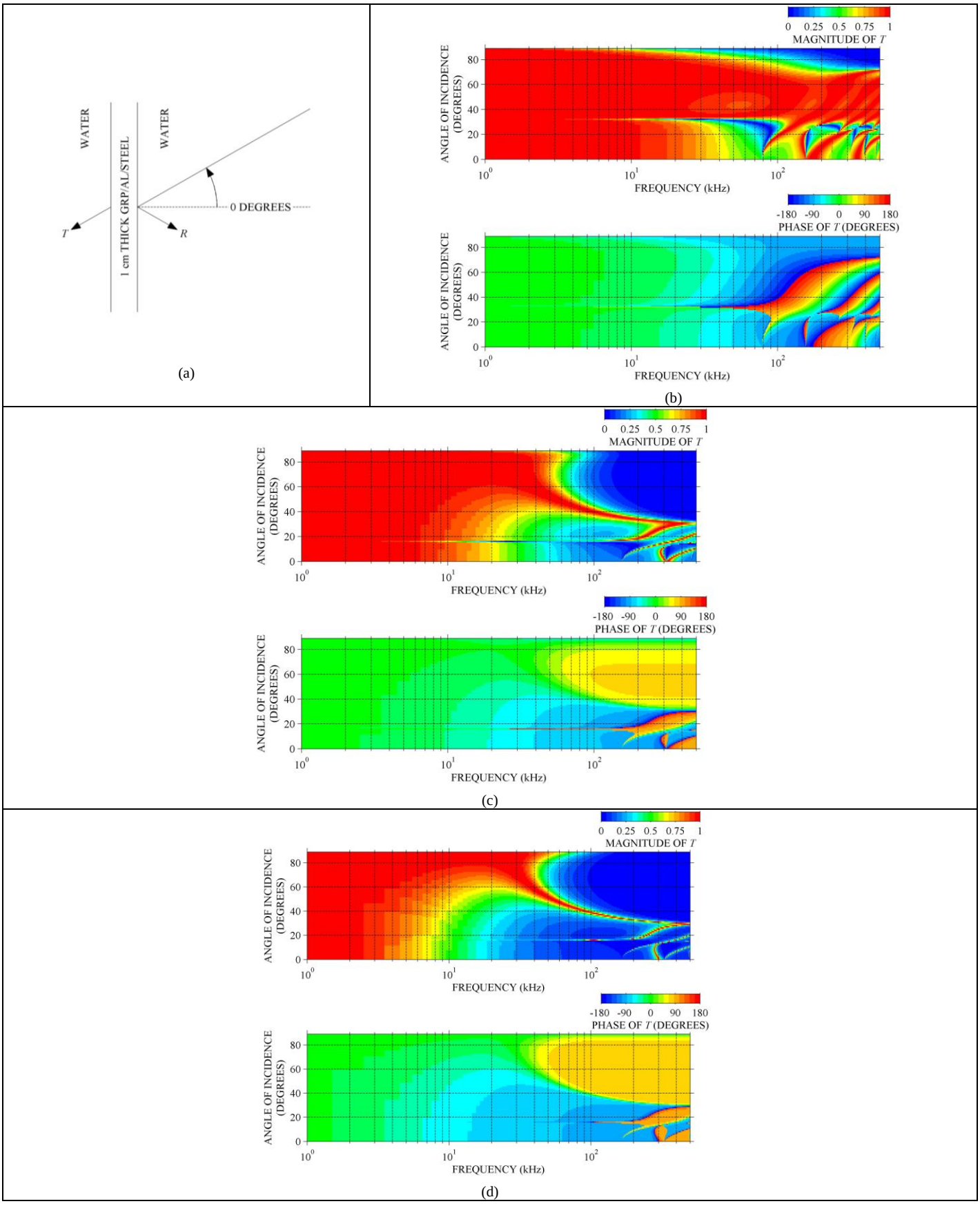

Fig. 3. In (a), the simplified target penetrability model based on plane-wave transmission coefficients (T); in (b), the T s for glass-reinforced plastic (GRP); in (c), for aluminium; in (d), for stainless steel.

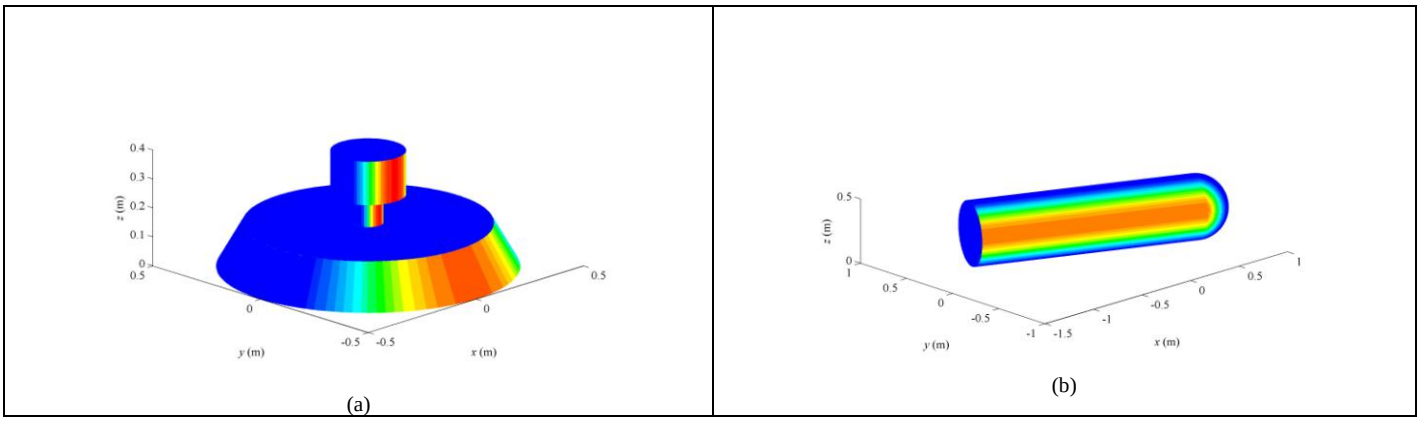

Fig. 4. The simplified target model for coherent scattering, based on plane-wave reflection coefficients $R = \pm 1$ (Kirchhoff approx.). In (a), the Manta mine, incident/scattered field at azimuth of 270 degrees and grazing angle of 10 degrees; in (b), the Murena mine, axis rotated to azimuth of 337.5 degrees, incident/scattered field at azimuth of 225 degrees and grazing angle of 10 degrees.

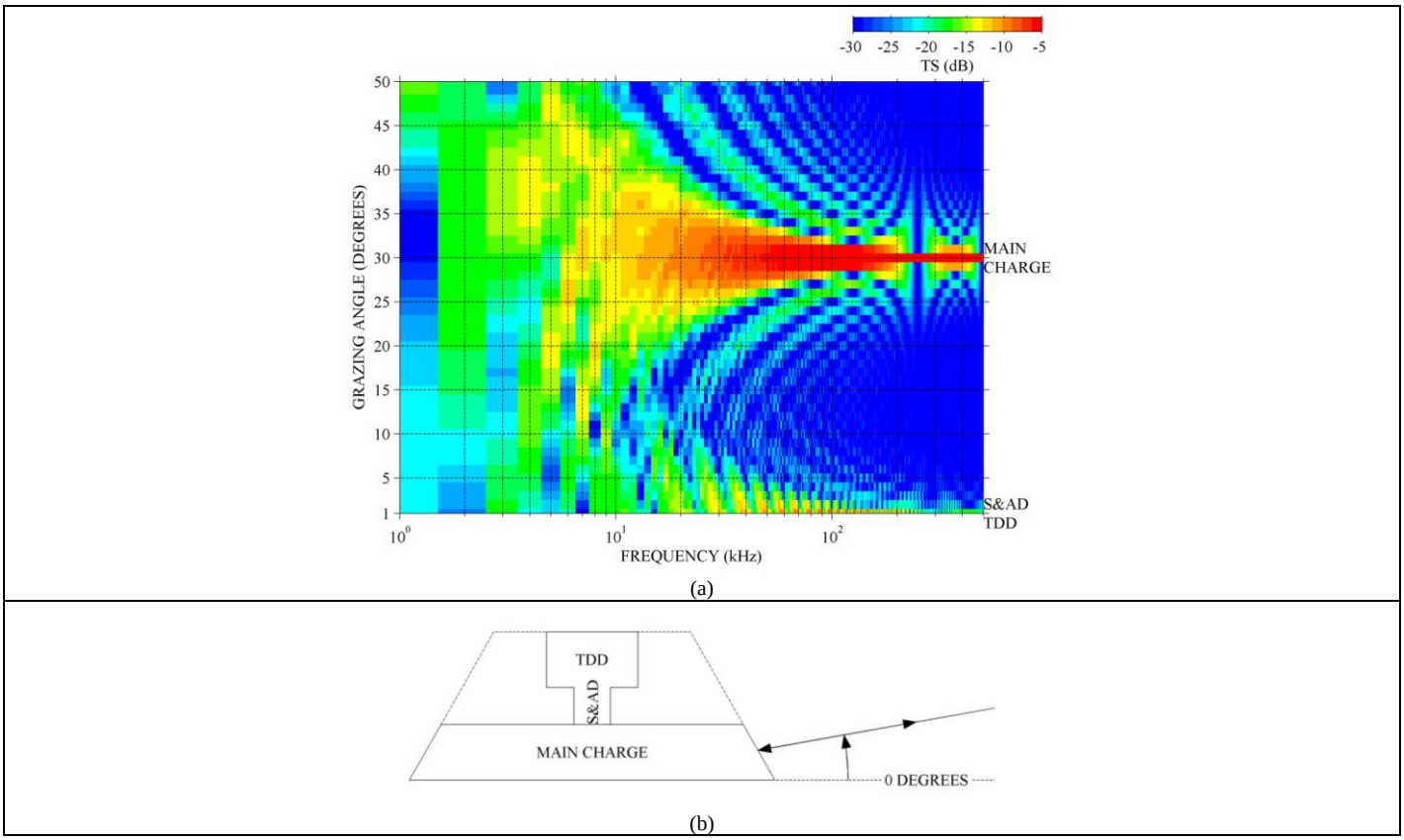

Fig. 5. In (a), target strengths TSs (monostatic), for the Manta mine, by means of the simplified target model for coherent scattering; in (b), schematic of the monostatic scattering.

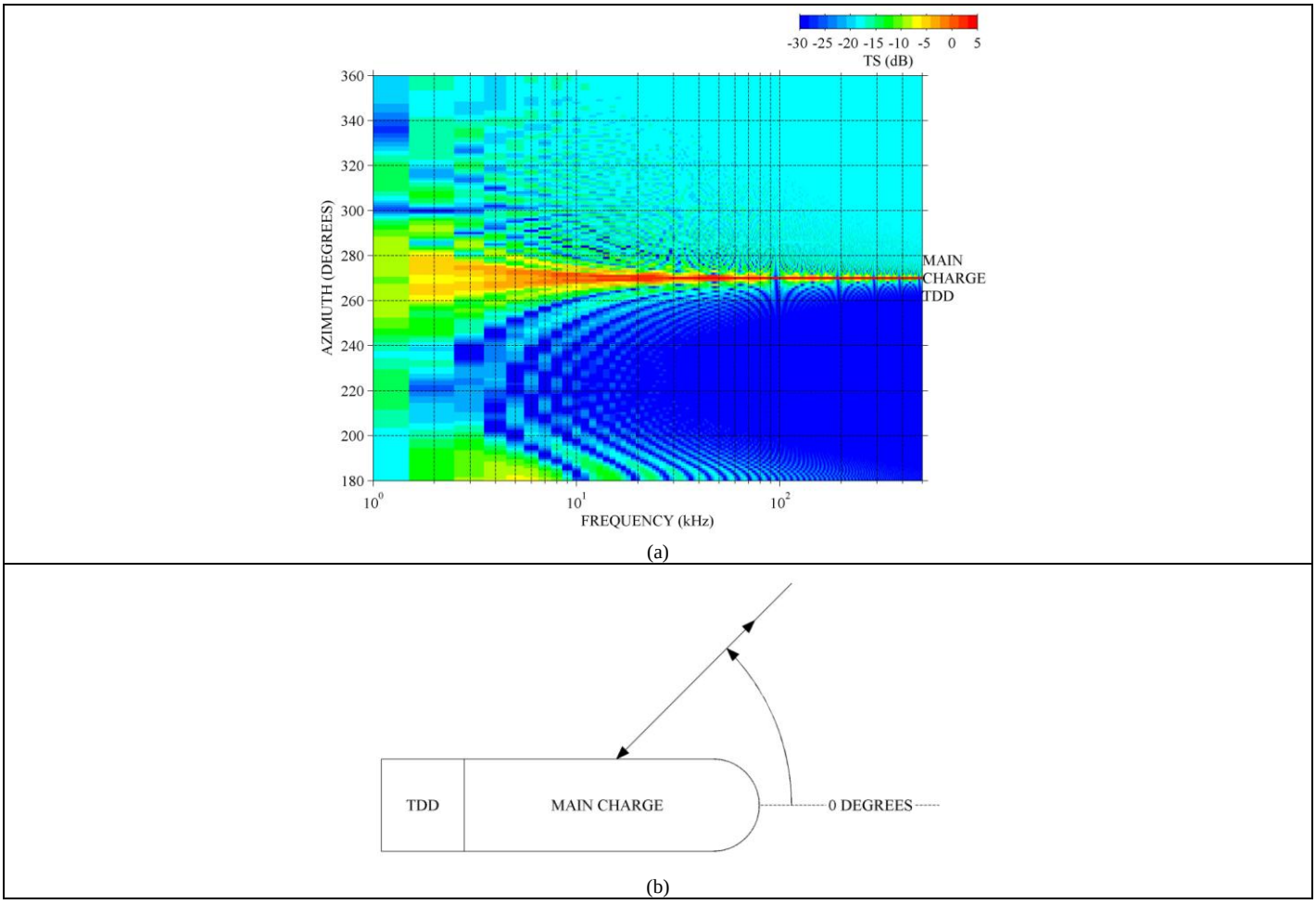

Fig. 6. In (a), target strengths TSs (monostatic), for the Murena mine, by means of the simplified target model for coherent scattering; in (b), schematic of the monostatic scattering.

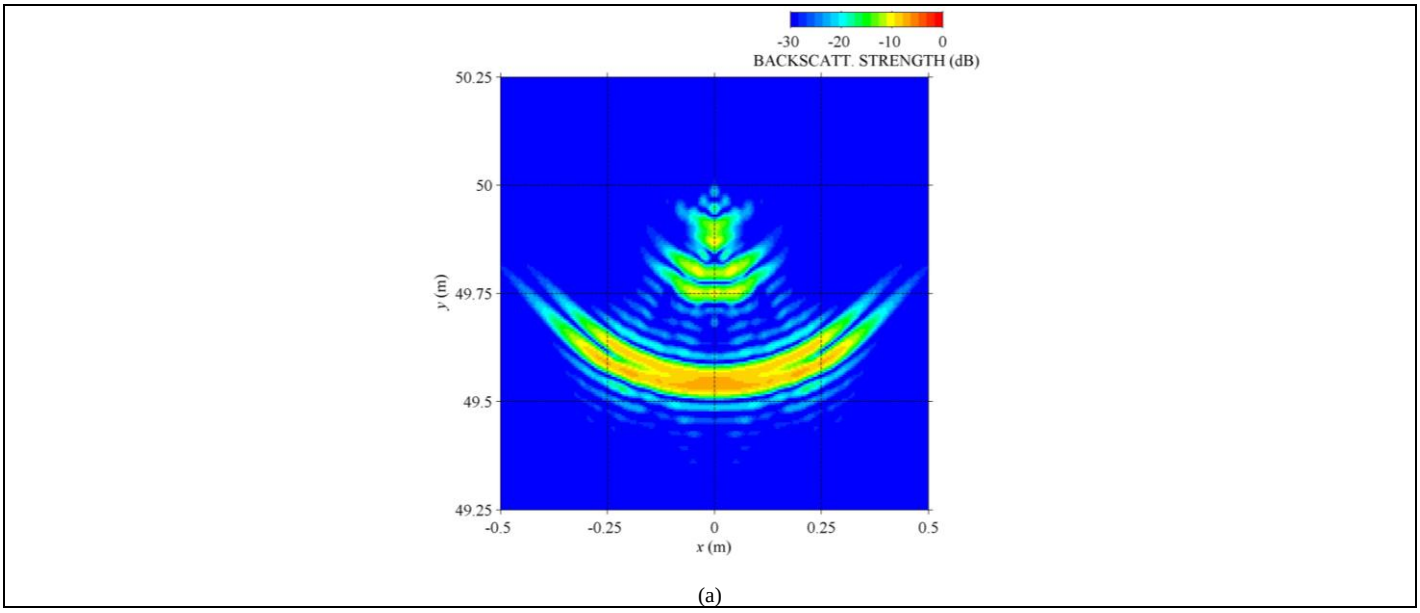

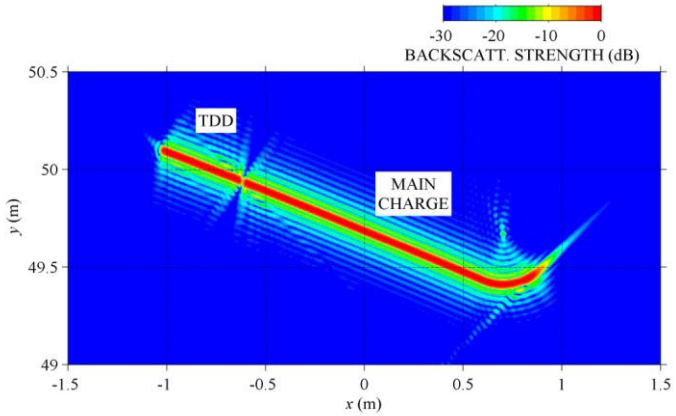

(b)

Fig. 7. The MPS system performance for Manta and Murena mine imagery. In (a), the Manta mine, incident/scattered field at grazing angle of 20 degrees; in (b), the Murena mine, incident/scattered field at grazing angle of 10 degrees.

Table 1. Comparison of LF system parameters.

System	Midband freq. $\frac{c}{\lambda_0}$ (kHz)	Bandwidth B (kHz)	Pulse type	Sector width Θ (degrees)	Resolution (cm × cm)
Contemp. LF	12	8	LFM (10 ms)	38	9 × 9
MPS	17.5	25	LFM (10 ms)	90	2.7 × 3

Table 2. Target echo-to-reverb. ratios at 10 (20) degrees grazing for Manta mine interior components (dB).

Component	R	Rock	Sand	Silt	Clay
Main charge	1[a]	7.5 (11.5)	15.5 (18)	20.5 (21.5)	24 (27.5)
TDD	-1	18 (9)	26 (15.5)	31 (19)	34.5 (25)
S&AD	-1	20 (9)	28 (15.5)	33 (19)	36.5 (25)

[a] $R = 0.4$, typically; accounted for by correction of -8 dB to ratios.

Table 3. Target echo-to-reverb. ratios at 10 degrees grazing for Murena mine interior components (dB).

Component	R	Rock	Sand	Silt	Clay
Main charge	1[a]	22	30	35	38.5
TDD	-1	22	30	35	38.5

[a] $R = 0.4$, typically; accounted for by correction of -8 dB to ratios.